New Pt→M (M = Ag, Tl) complexes based on anionic cyclometalated Pt(II) complexes

*David Campillo, Úrsula Belío, and Antonio Martín**

Instituto de Síntesis Química y Catálisis Homogénea (ISQCH). Departamento de Química Inorgánica. Universidad de Zaragoza – CSIC. 50009 Zaragoza, Spain.

SUPPORTING INFORMATION

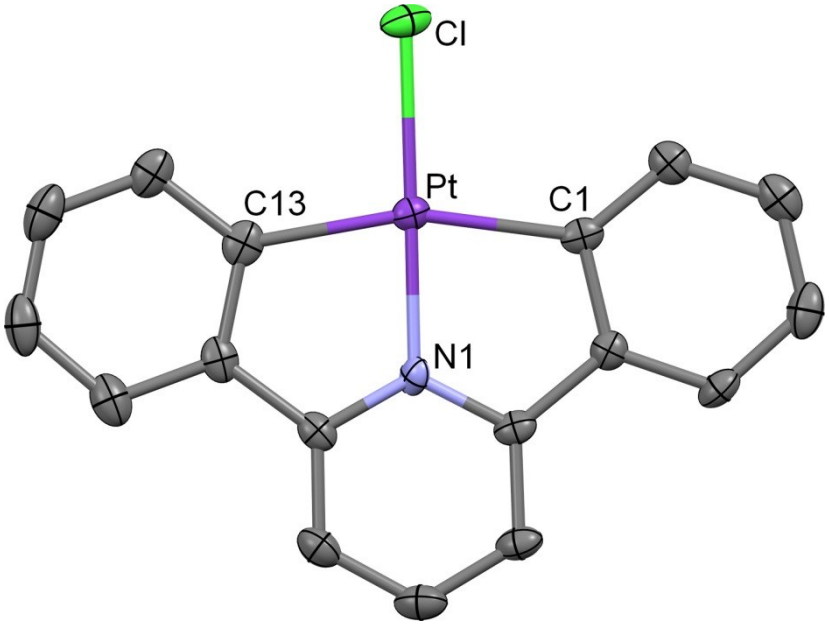

Figure S1. X-ray crystal structure of the anion of the complex (NBu_4)[Pt(CNC)Cl] (**1**).

Table S1. Relevant bond distances (Å) and angles (º) for the complex (NBu_4)[Pt(CNC)Cl] (**1**)

Pt−N(1)	1.958(4)	Pt−C(13)	2.056(4)
Pt−C(1)	2.077(4)	Pt−Cl	2.3198(14)
N(1)−Pt−C(13)	81.15(18)	N(1)−Pt−C(1)	81.35(17)
C(13)−Pt−C(1)	162.40(15)	N(1)−Pt−Cl	179.25(14)
C(13)−Pt−Cl	98.45(12)	C(1)−Pt−Cl	99.03(11)

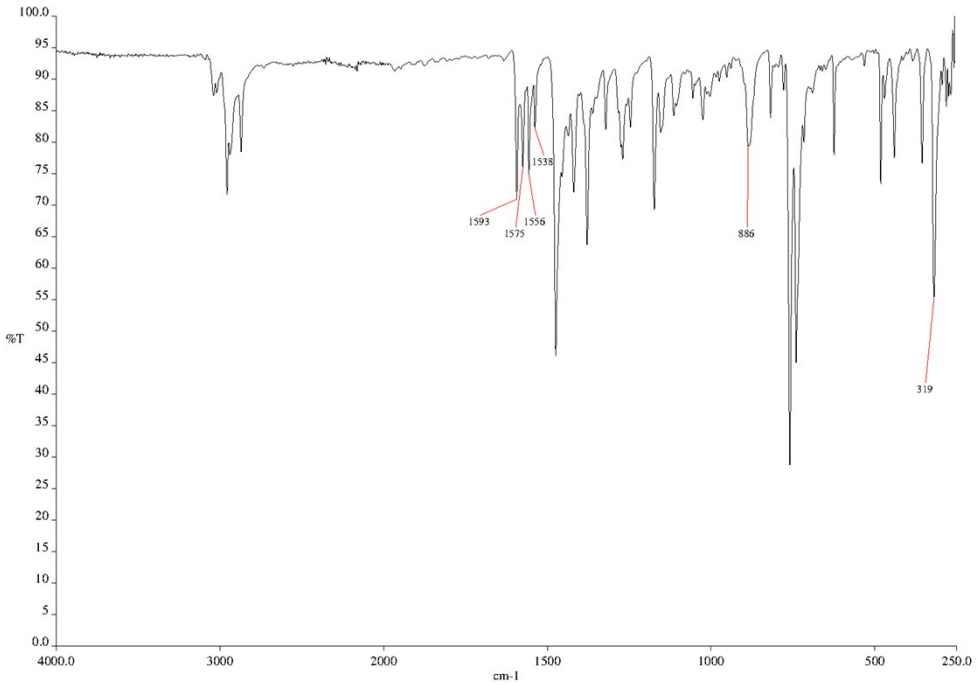

Figure S2. IR spectrum of complex (NBu_4)[Pt(CNC)Cl] (**1**).

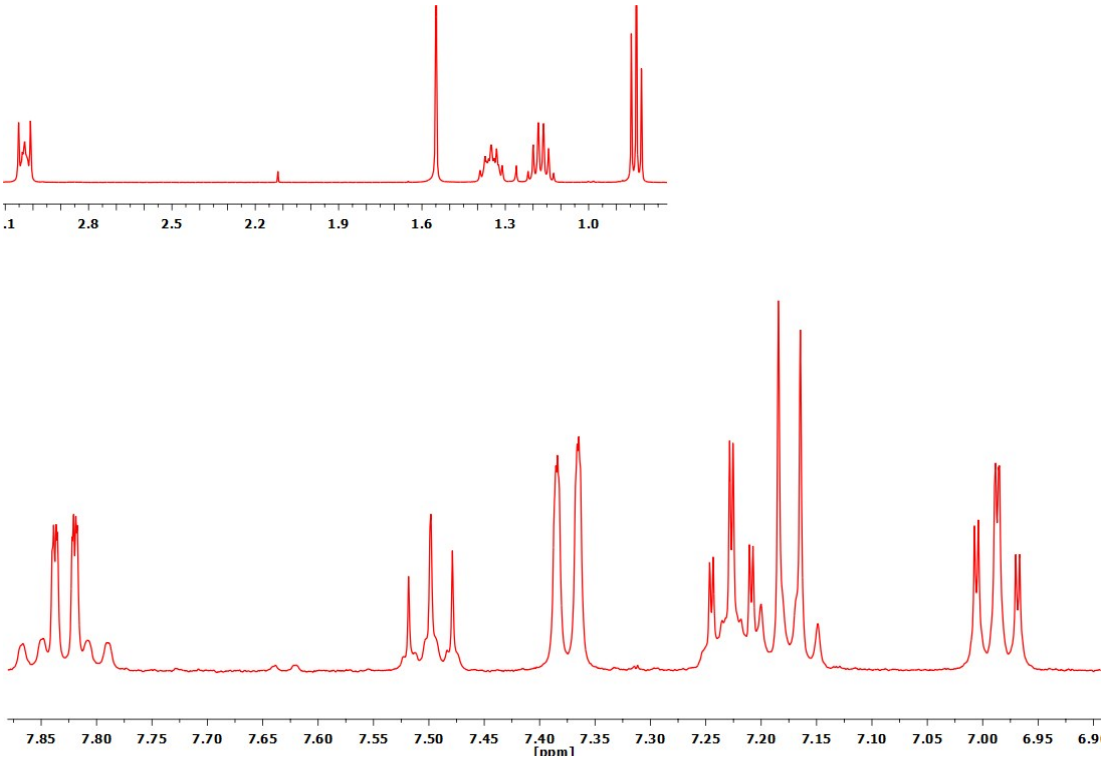
.1
2.8
2.5
2.2
1.9
1.6
1.3
1.0
7.85
7.80
7.75
7.70
7.65
7.60
7.55
7.50
7.45
7.40
7.35
7.30
7.25
7.20
7.15
7.10
7.05
7.00
6.95
[ppm]

(a)

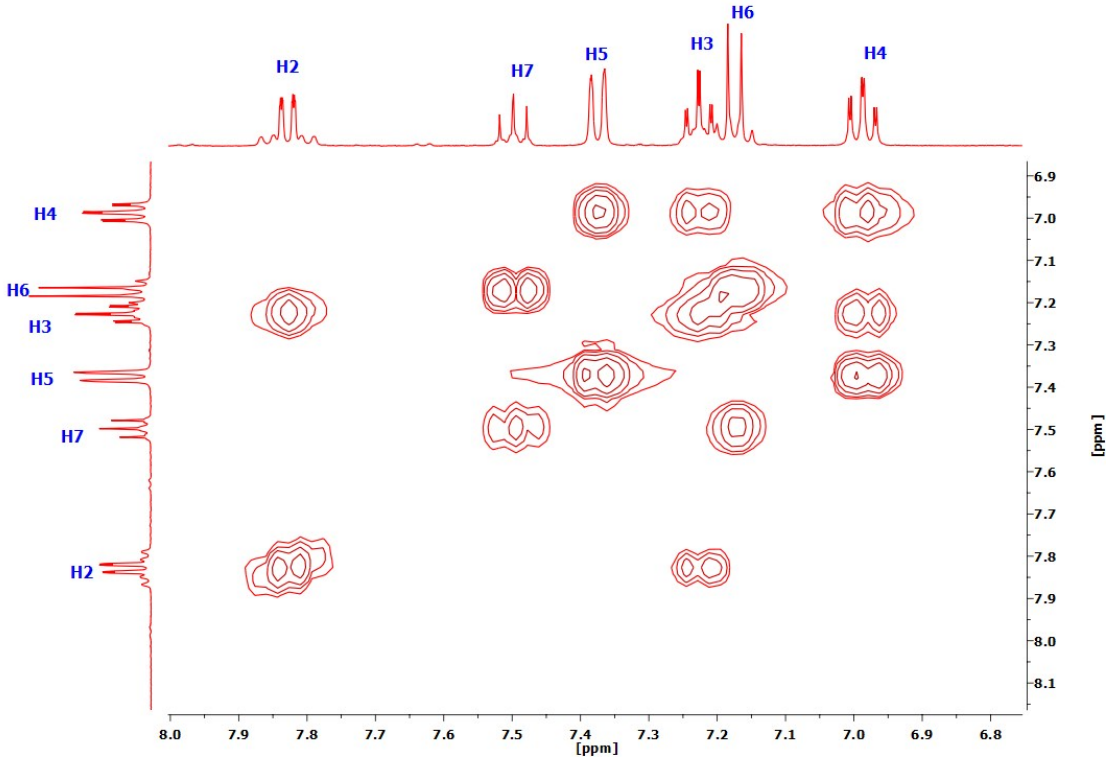
H2
H7
H5
H3
H6
H4
H4
H6
H3
H5
H7
H2
8.0
7.9
7.8
7.7
7.6
7.5
7.4
7.3
7.2
7.1
7.0
6.9
6.8
[ppm]
6.9
7.0
7.1
7.2
7.3
7.4
7.5
7.6
7.7
7.8
7.9
8.0
8.1
[ppm]

(b)

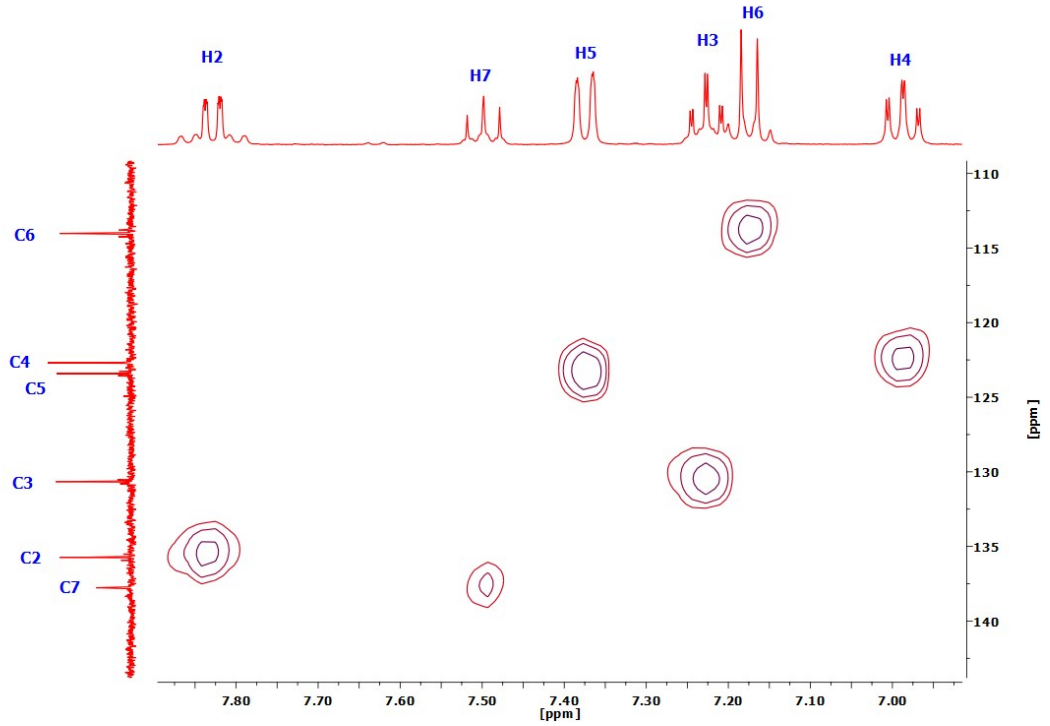
H2
H7
H5
H3
H6
H4
C6
C4
C5
C3
C2
C7
[ppm]

(c)

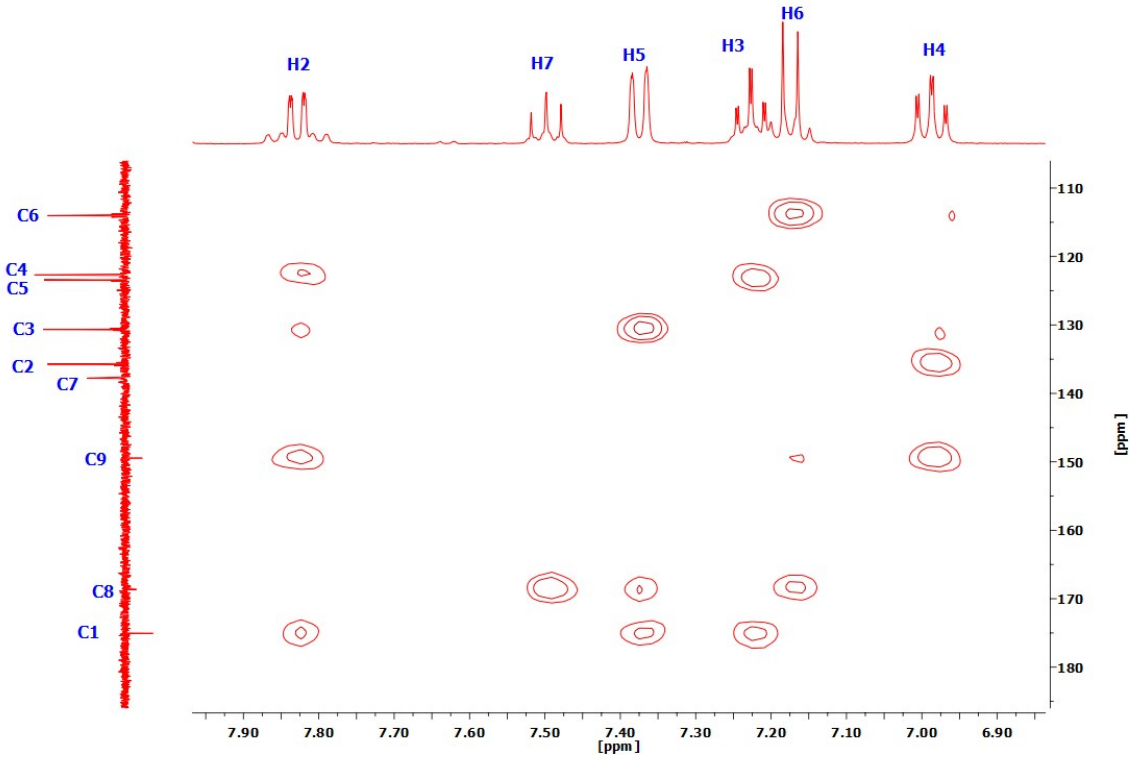
H2
H7
H5
H3
H6
H4
C6
C4
C5
C3
C2
C7
C9
C8
C1
[ppm]

(d)

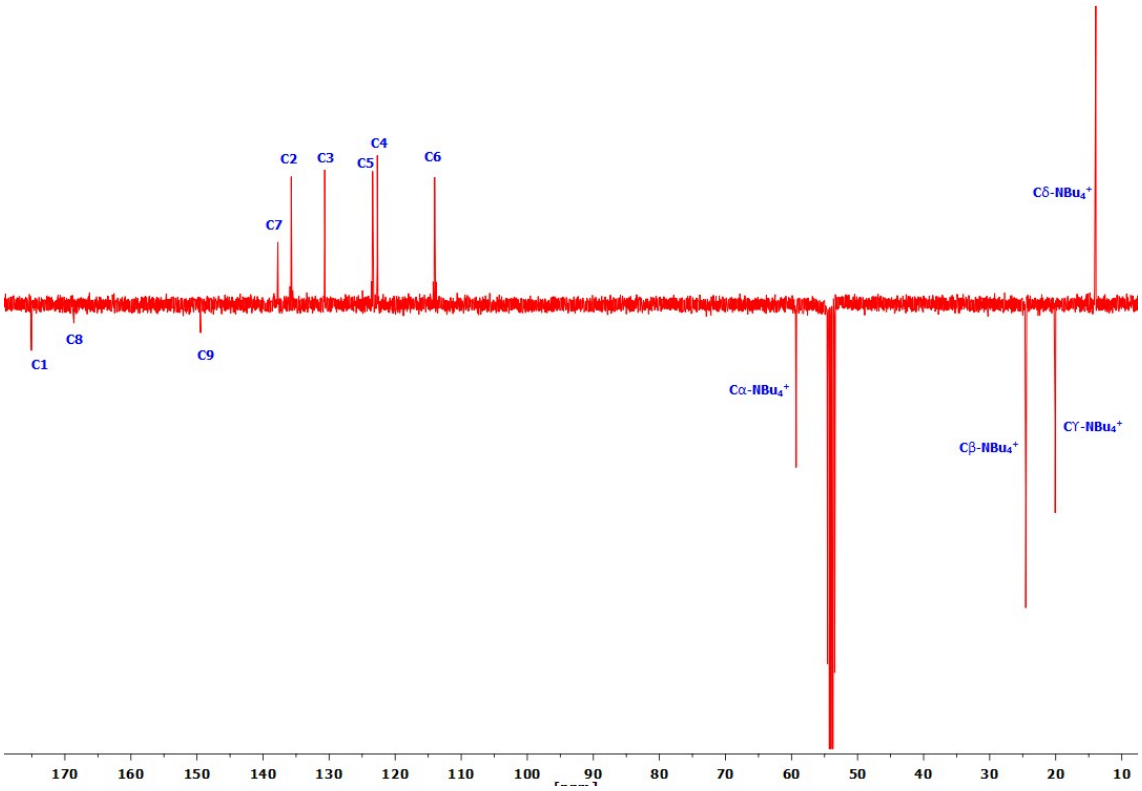

(e)

Figure S3. ^{1}H NMR (a), COSY ^{1}H-^{1}H (b), ^{1}H-^{13}C HSQC (c), ^{1}H-^{13}C HMBC (d) and APT (e) spectra of complex (NBu_4)[Pt(CNC)Cl] (**1**) in CD_2Cl_2 at RT.

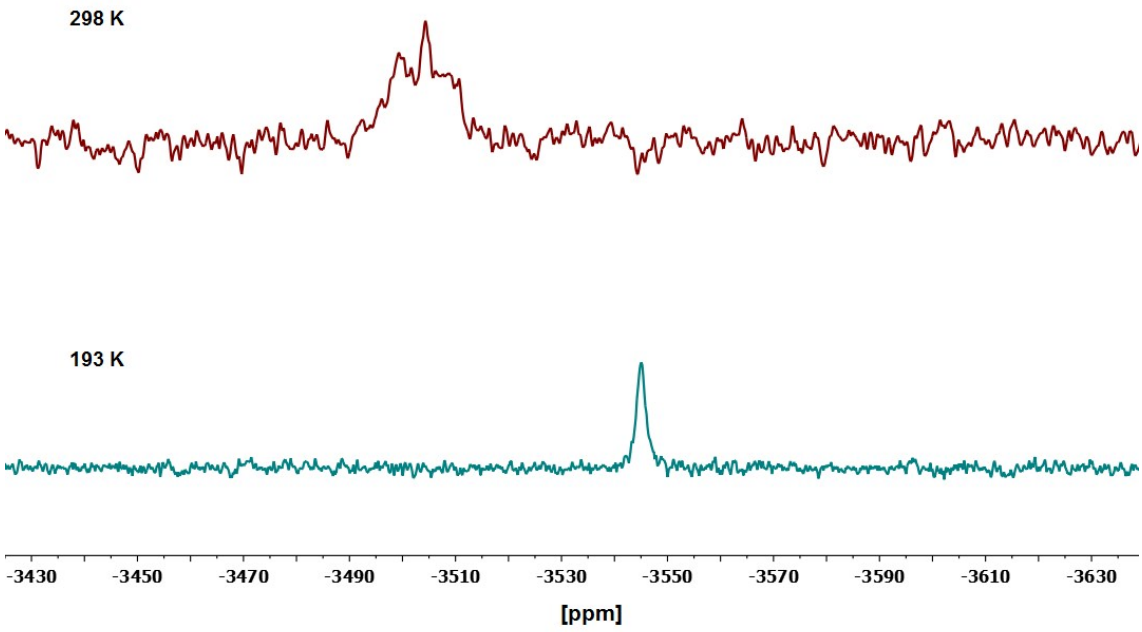

Figure S4. $^{195}Pt\{^{1}H\}$ NMR in CD_2Cl_2 at 298 K and 193K of complex (NBu_4)[Pt(CNC)Cl] (**1**).

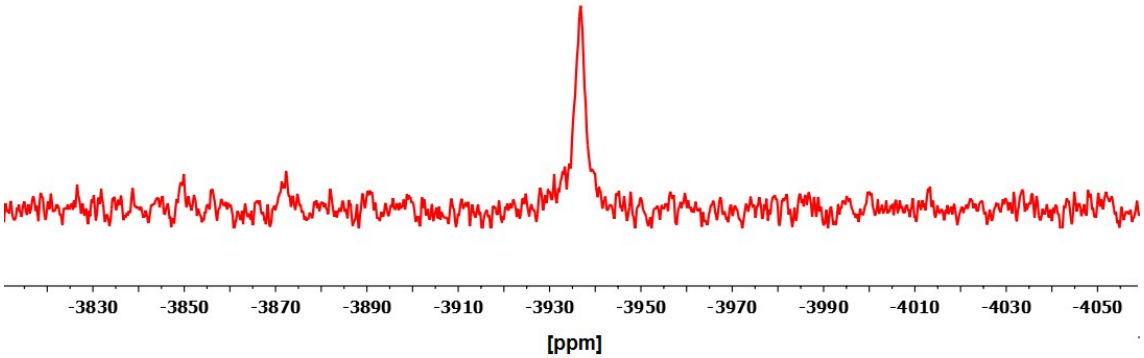

Figure S5. $^{195}Pt\{^{1}H\}$ RMN in dmso-d_6 at 298 K of complex (NBu_4)[Pt(CNC)Cl] (**1**).

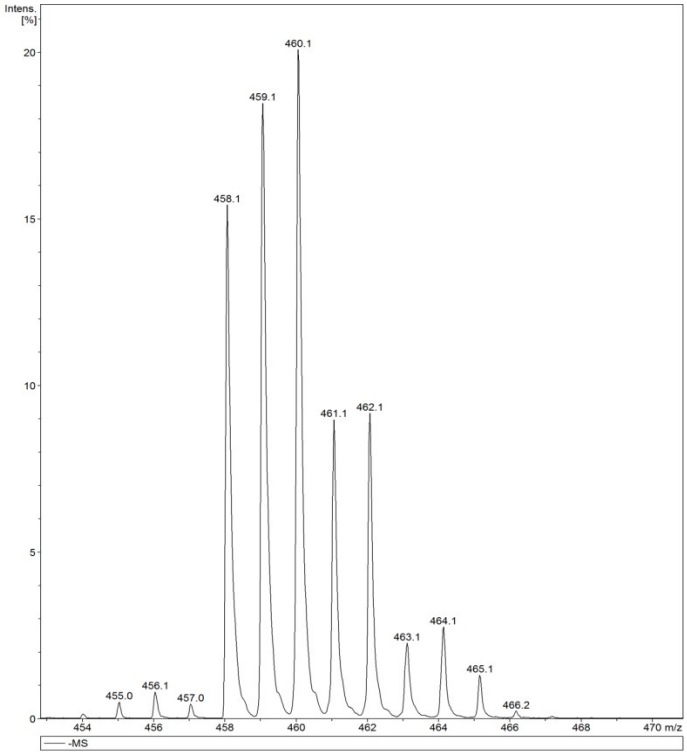

Figure S6. MS-MALDI- (DIT) peak of complex (NBu_4)[Pt(CNC)Cl] (**1**).

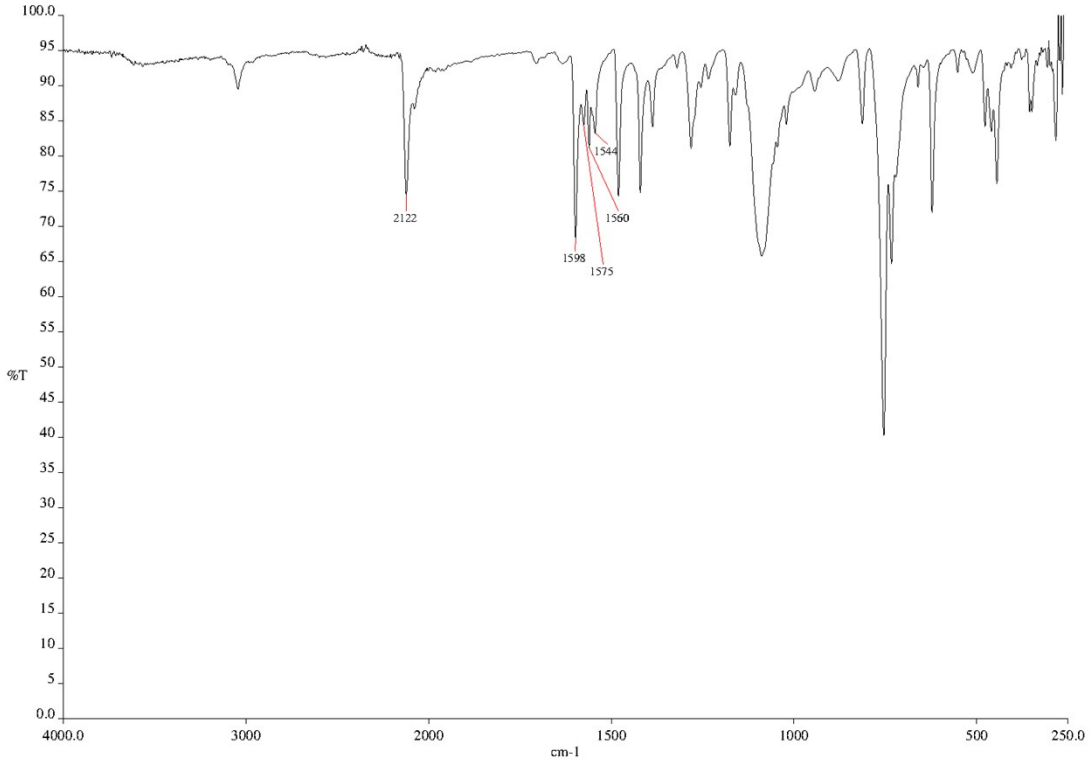

Figure S7. IR spectrum of compound [PtAg(CNC)(CN)] (**4**)

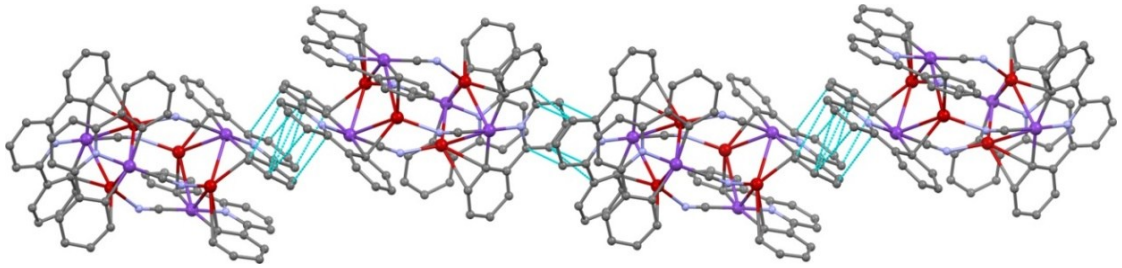

Figure S8. Supramolecular arrangement found in the crystal structure of [{Pt(CNC)(μ-CN)}$_4$Ag$_4$] (**4**) showing the π···π intermolecular interactions.

Table S2**.** Relevant bond distances (Å) and angles (º) for the complex [{Pt(CNC)(μ-CN)}$_4$Ag$_4$] (**4**)**.**

Ag(1)−N(2D)	2.222(5)	Ag(1)−C(7Z)	2.412(17)
Ag(1)−C(7B)	2.466(14)	Ag(1)−C(7A)	2.483(6)
Ag(1)−Pt(1Z)	2.667(2)	Ag(1)−Pt(1A)	2.8792(5)
Ag(1)−Pt(1B)	3.0408(19)	Ag(2)−N(2C)	2.248(6)
Ag(2)−C(13Z)	2.481(12)	Ag(2)−C(13A)	2.499(6)
Ag(2)−C(13B)	2.527(14)	Ag(2)−Pt(1B)	2.7740(11)
Ag(2)−Pt(1A)	2.8819(5)	Ag(2)−Pt(1Z)	3.0005(18)
Ag(3)−N(2A)	2.209(5)	Ag(3)−C(13D)	2.503(5)
Ag(3)−C(13C)	2.577(5)	Ag(3)−Pt(1C)	2.7869(4)
Ag(3)−Pt(1D)	2.9460(5)	Ag(3)−Ag(4)	3.3580(6)
Ag(4)−N(2B)	2.11(3)	Ag(4)−N(2Z)	2.31(2)
Ag(4)−C(7C)	2.501(6)	Ag(4)−C(7D)	2.539(5)
Ag(4)−Pt(1D)	2.8046(5)	Ag(4)−Pt(1C)	2.9088(5)
Pt(1A)−C(18A)	1.939(6)	Pt(1A)−N(1A)	2.004(4)
Pt(1A)−C(7A)	2.072(5)	Pt(1A)−C(13A)	2.073(5)
C(18A)−N(2A)	1.156(6)	Pt(1B)−C(18B)	1.940(10)
Pt(1B)−N(1B)	2.002(8)	Pt(1B)−C(7B)	2.067(9)
Pt(1B)−C(13B)	2.085(10)	C(18B)−N(2B)	1.182(13)
Pt(1Z)−C(18Z)	1.928(10)	Pt(1Z)−N(1Z)	2.010(9)
Pt(1Z)−C(13Z)	2.071(10)	Pt(1Z)−C(7Z)	2.083(10)
C(18Z)−N(2Z)	1.187(12)	Pt(1C)−C(18C)	1.956(7)
Pt(1C)−N(1C)	2.009(5)	Pt(1C)−C(7C)	2.073(6)
Pt(1C)−C(13C)	2.073(5)	Pt(1D)−C(18D)	1.946(6)
Pt(1D)−N(1D)	2.007(5)	Pt(1D)−C(7D)	2.065(6)
Pt(1D)−C(13D)	2.084(6)	N(2C)−C(18C)	1.143(7)
N(2D)−C(18D)	1.153(7)		
Pt(1Z)−Ag(1)−Pt(1A)	95.80(3)	Pt(1A)−Ag(1)−Pt(1B)	93.35(2)
Pt(1B)−Ag(2)−Pt(1A)	99.21(5)	Pt(1A)−Ag(2)−Pt(1Z)	88.83(5)
Pt(1C)−Ag(3)−Pt(1D)	96.235(13)	Pt(1D)−Ag(4)−Pt(1C)	96.695(14)
N(2B)−Ag(4)−Ag(3)	116.5(11)	N(2Z)−Ag(4)−Ag(3)	110.6(9)
C(7C)−Ag(4)−Ag(3)	93.29(13)	C(7D)−Ag(4)−Ag(3)	101.33(13)

C(8C)−Ag(4)−Ag(3)	121.91(14)	Pt(1D)−Ag(4)−Ag(3)	56.255(11)
Pt(1C)−Ag(4)−Ag(3)	52.211(10)	Ag(1)−Pt(1A)−Ag(2)	74.489(15)
Ag(2)−Pt(1B)−Ag(1)	73.52(3)	Ag(1)−Pt(1Z)−Ag(2)	75.68(3)
Ag(3)−Pt(1C)−Ag(4)	72.217(13)	Ag(4)−Pt(1D)−Ag(3)	71.408(13)

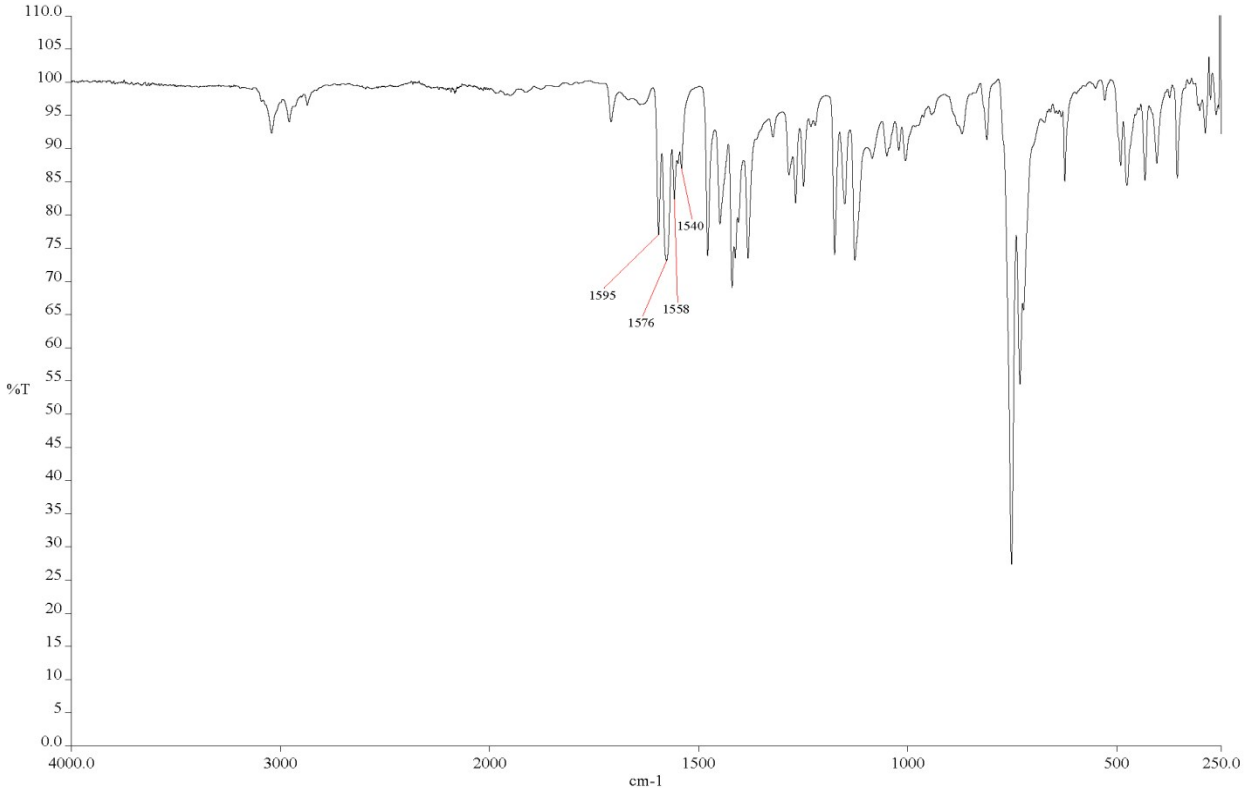

Figure S9. IR spectrum of the solid [PtAg(CNC)(S-2py)] (**5**)

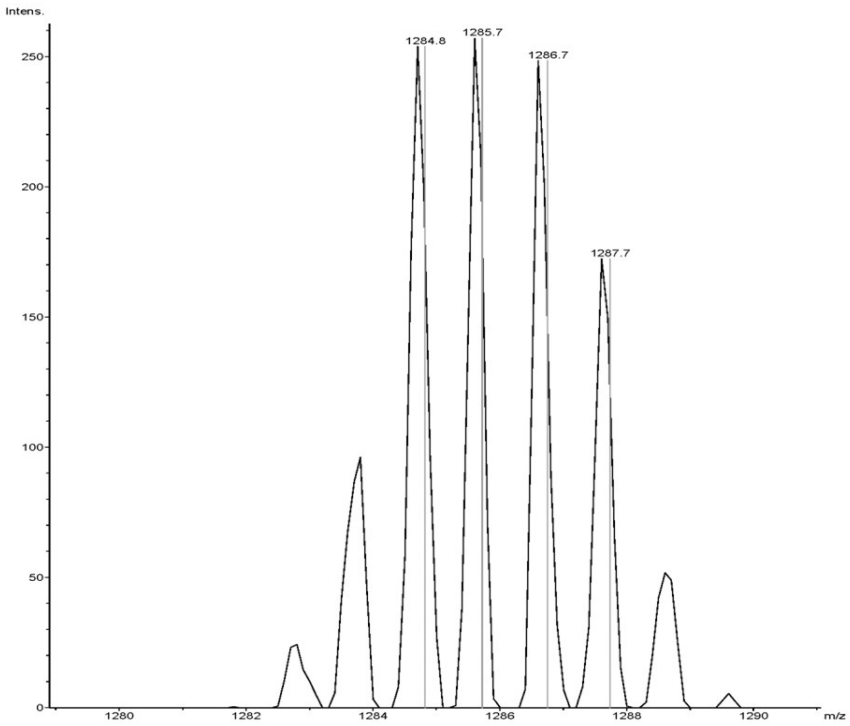

Figure S10. MS-ESI+ peak found for [PtAg(CNC)(S-2py)] (**5**). This peak corresponds to $[\{Pt(CNC)(S\text{-}2Py)\}_2Ag_2]+H^+$.

Table S3. Relevant bond distances (Å) and angles (º) for the complex $[\{Pt(CNC)(S\text{-}2py)\}_2Ag_2]$ (**5**)**.**

Pt(1)−N(1)	1.960(7)	Pt(1)−N(2)	2.051(6)
Pt(1)−C(13)	2.067(8)	Pt(1)−C(7)	2.084(8)
Pt(1)−Ag(2)	2.8659(7)	Pt(1)−Ag(1)	3.0360(7)
Pt(2)−N(3)	1.991(6)	Pt(2)−C(35)	2.063(8)
Pt(2)−C(29)	2.085(7)	Pt(2)−S(2)	2.282(2)
Pt(2)−Ag(2)	2.8237(7)	Pt(2)−Ag(1)	3.0380(7)
Ag1−N(4)	2.174(6)	Ag1−S(1)	2.422(2)
Ag1−Ag(2)	2.8910(8)	Ag2−C(29)	2.355(8)
Ag2−C(7)	2.386(8)	Ag2−S(1)	2.601(2)
N(1)−Pt(1)−N(2)	176.3(3)	N(1)−Pt(1)−C(13)	81.5(3)
N(2)−Pt(1)−C(13)	99.1(3)	N(1)−Pt(1)−C(7)	81.0(3)
N(2)−Pt(1)−C(7)	98.3(3)	C(13)−Pt(1)−C(7)	162.4(3)

Ag2−Pt(1)−Ag(1)	58.576(17)	N(3)−Pt(2)−C(35)	80.4(3)
N(3)−Pt(2)−C(29)	79.9(3)	C(35)−Pt(2)−C(29)	159.7(3)
N(3)−Pt(2)−S(2)	173.00(19)	C(35)−Pt(2)−S(2)	106.6(2)
C(29)−Pt(2)−S(2)	93.1(2)	Ag2−Pt(2)−Ag(1)	58.968(17)

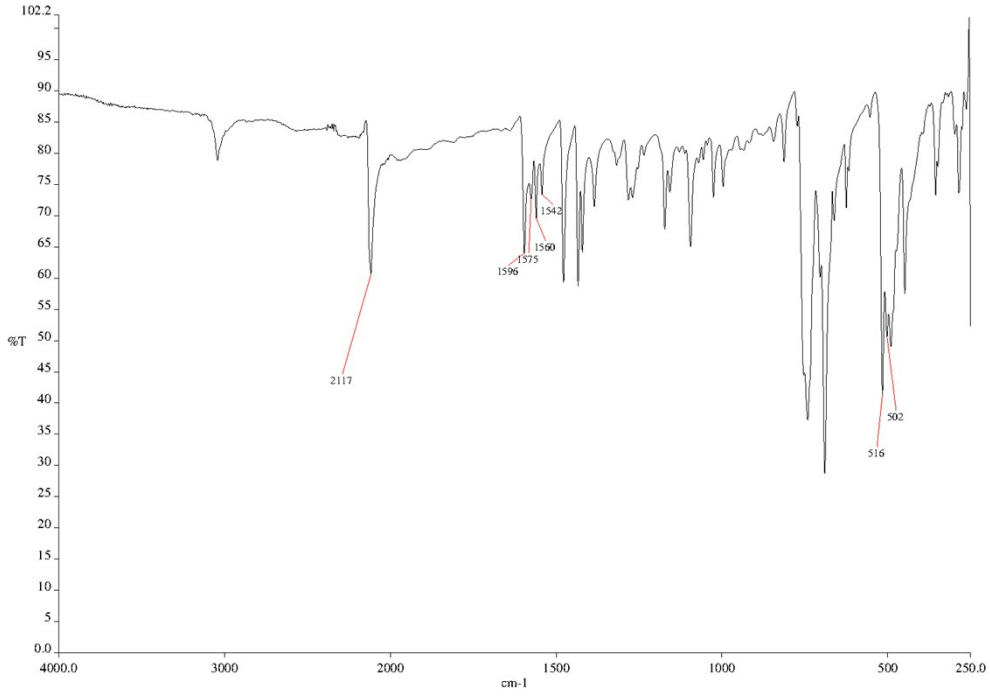

Figure S11. IR spectrum of [Pt(CNC)(CN)Ag(PPh_3)] (**6**)

Table S4. Relevant bond distances (Å) and angles (º) for the complex [{Pt(CNC)(μ-CN)}$_2${Ag(PPh$_3$)}$_2$] (**6**).

Pt(1)−C(18)	1.930(7)	Pt(1)−N(1)	2.006(5)
Pt(1)−C(13)	2.058(5)	Pt(1)−C(7)	2.088(6)
Pt(1)−Ag(1)	2.9055(5)	Pt(2)−C(54)	1.932(7)
Pt(2)−N(3)	2.007(5)	Pt(2)−C(49)	2.055(6)
Pt(2)−C(43)	2.070(6)	Pt(2)−Ag(2)	2.8652(5)
Ag(1)−N(4)	2.181(5)	Ag(1)−P(1)	2.3947(17)
Ag(1)−C(7)	2.509(5)	Ag(2)−N(2)	2.181(5)
Ag(2)−P(2)	2.3780(17)	Ag(2)−C(43)	2.586(6)
N(2)−C(18)	1.159(8)	N(4)−C(54)	1.172(8)
C(18)−Pt(1)−N(1)	177.6(2)	C(18)−Pt(1)−C(13)	96.5(2)
N(1)−Pt(1)−C(13)	81.4(2)	C(18)−Pt(1)−C(7)	101.5(2)
N(1)−Pt(1)−C(7)	80.6(2)	C(13)−Pt(1)−C(7)	161.9(2)
C(54)−Pt(2)−N(3)	177.4(2)	C(54)−Pt(2)−C(49)	97.2(2)
N(3)−Pt(2)−C(49)	81.2(2)	C(54)−Pt(2)−C(43)	101.5(2)
N(3)−Pt(2)−C(43)	80.2(2)	C(49)−Pt(2)−C(43)	161.3(2)
N(4)−Ag(1)−P(1)	130.43(14)	N(4)−Ag(1)−Pt(1)	107.01(13)
P(1)−Ag(1)−Pt(1)	116.08(4)	N(2)−Ag(2)−P(2)	133.77(14)
N(2)−Ag(2)−Pt(2)	115.56(14)	P(2)−Ag(2)−Pt(2)	108.64(4)
C(18)−N(2)−Ag(2)	151.9(5)	C(54)−N(4)−Ag(1)	167.0(5)
N(2)−C(18)−Pt(1)	178.1(6)	N(4)−C(54)−Pt(2)	177.8(6)

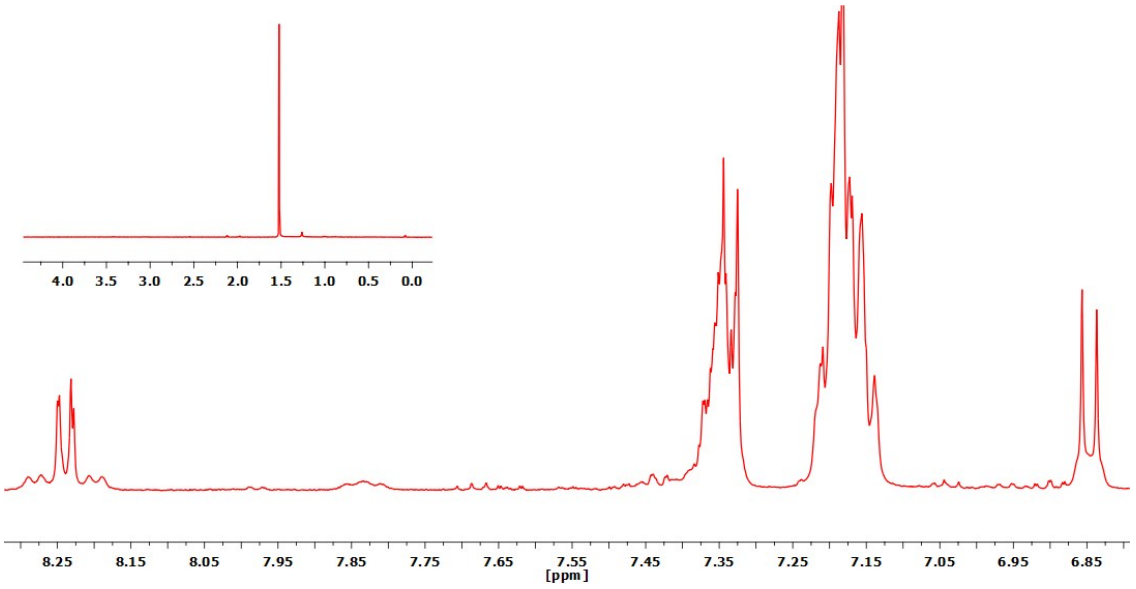
4.0 3.5 3.0 2.5 2.0 1.5 1.0 0.5 0.0
8.25 8.15 8.05 7.95 7.85 7.75 7.65 7.55 7.45 7.35 7.25 7.15 7.05 6.95 6.85
[ppm]

(a)

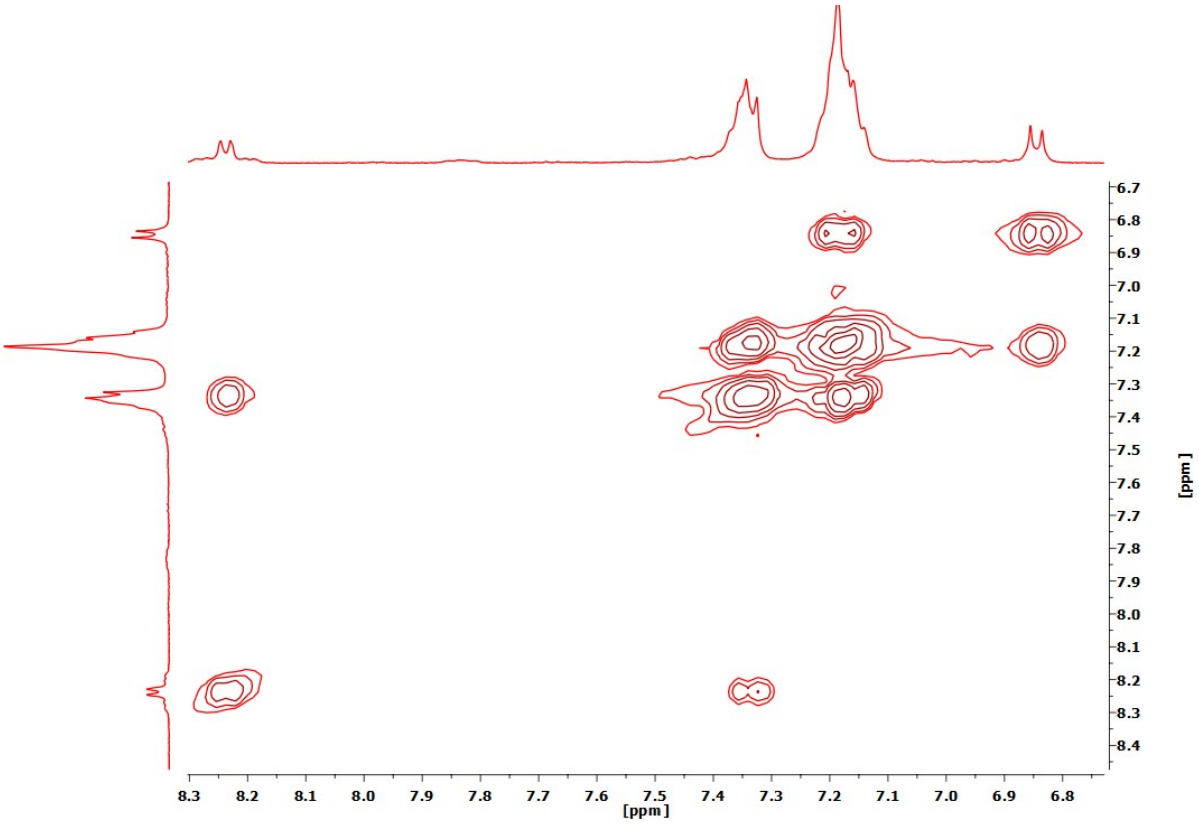
6.7 6.8 6.9 7.0 7.1 7.2 7.3 7.4 7.5 7.6 7.7 7.8 7.9 8.0 8.1 8.2 8.3 8.4
[ppm]
8.3 8.2 8.1 8.0 7.9 7.8 7.7 7.6 7.5 7.4 7.3 7.2 7.1 7.0 6.9 6.8
[ppm]

(b)

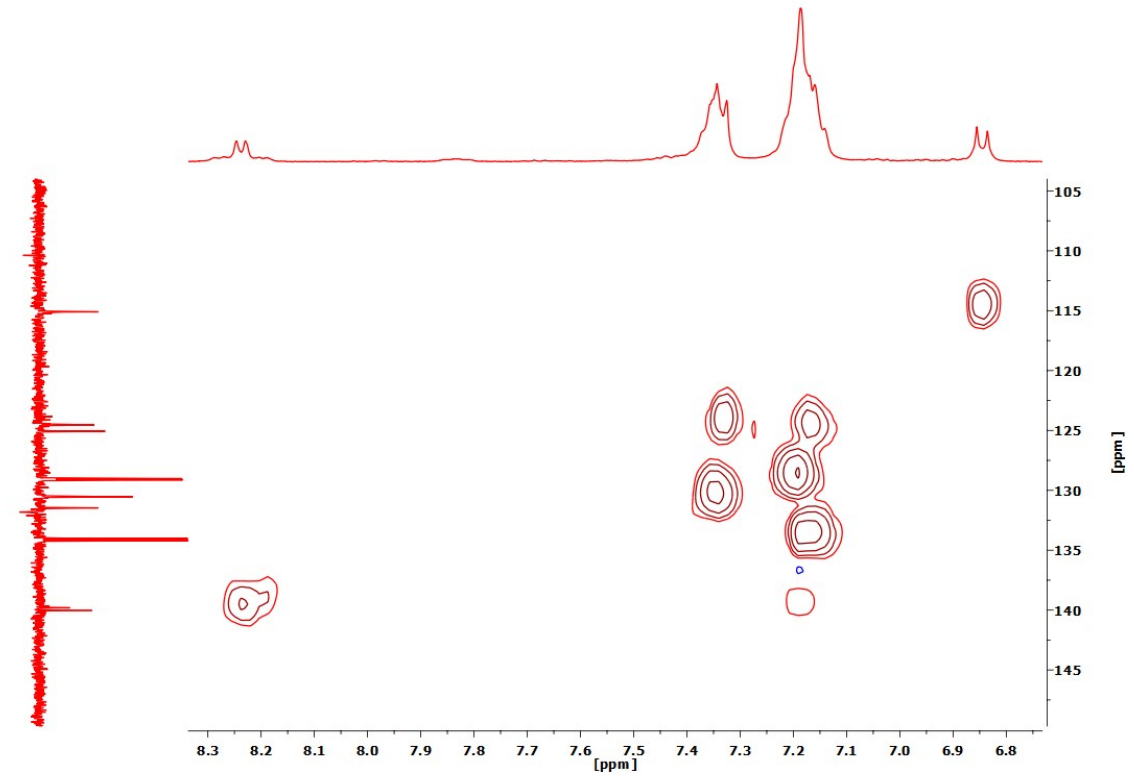
105
110
115
120
125
130
135
140
145
[ppm]
8.3
8.2
8.1
8.0
7.9
7.8
7.7
7.6
7.5
7.4
7.3
7.2
7.1
7.0
6.9
6.8
[ppm]

(c)

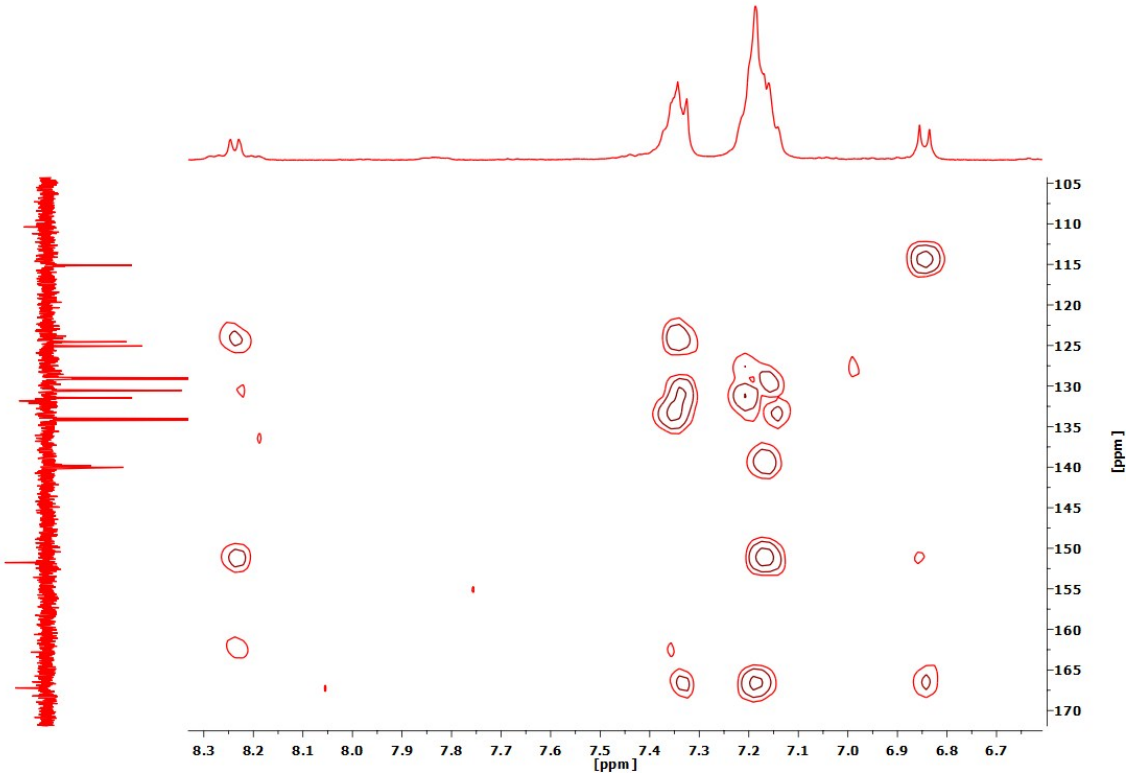
105
110
115
120
125
130
135
140
145
150
155
160
165
170
[ppm]
8.3
8.2
8.1
8.0
7.9
7.8
7.7
7.6
7.5
7.4
7.3
7.2
7.1
7.0
6.9
6.8
6.7
[ppm]

(d)

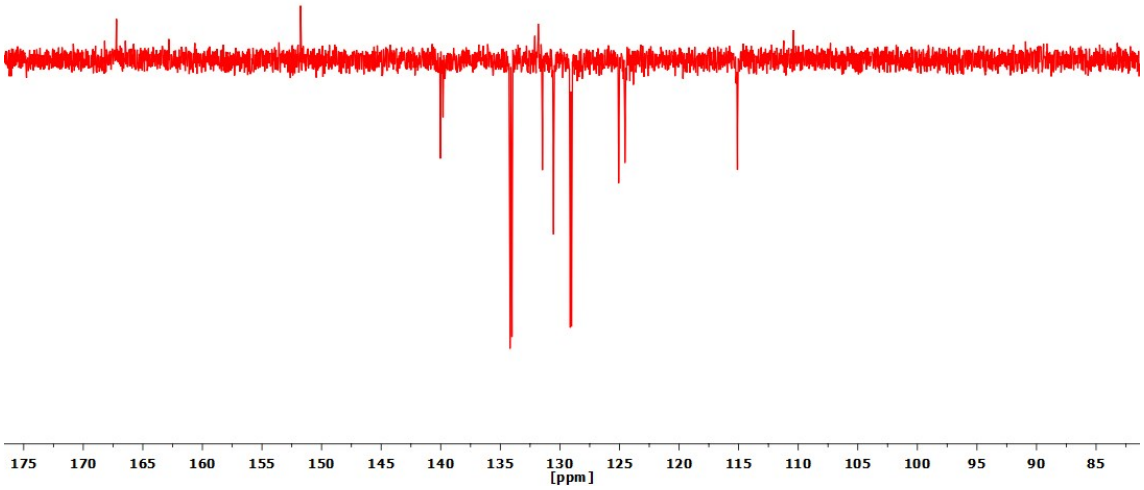

(e)

Figure S12. ^{1}H NMR (a), COSY ^{1}H-^{1}H (b), ^{1}H-^{13}C HSQC (c), ^{1}H-^{13}C HMBC (d) and APT (e) spectra of solutions of [Pt(CNC)(CN)Ag(PPh_3)] (**6**) in CD_2Cl_2 at RT.

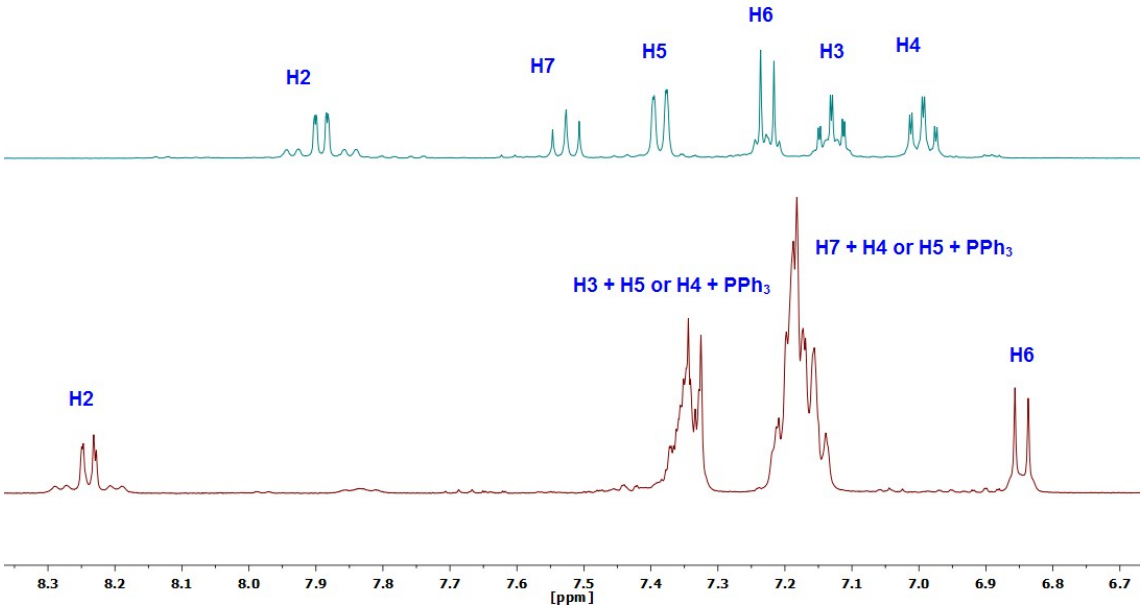

Figure S13. Aromatic region of the ^{1}H NMR spectra (CD_2Cl_2, room temperature) of (NBu_4)[Pt(CNC)(CN)] (**2**) (above) and [Pt(CNC)(CN)Ag(PPh_3)] (**6**) (below).

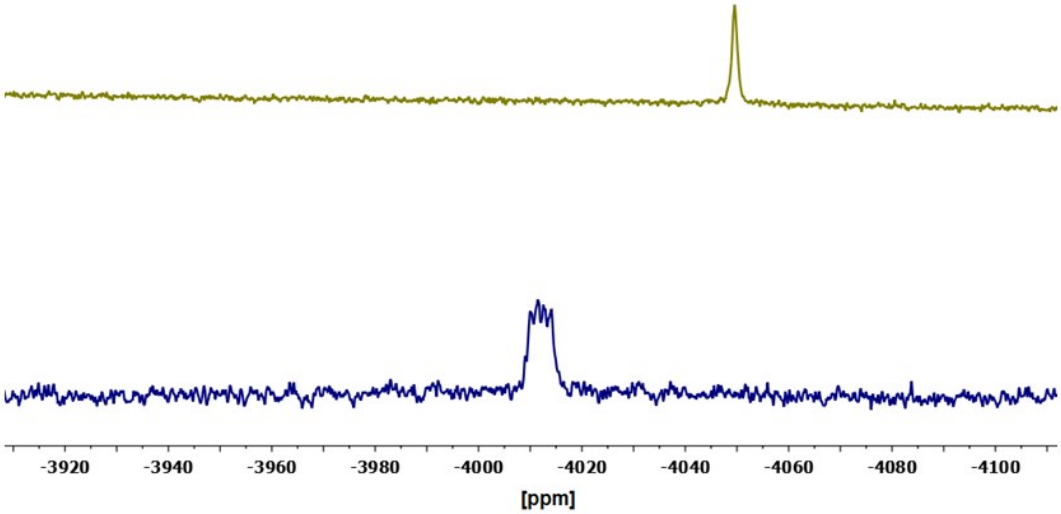

Figure S14.^{195}Pt {^{1}H} NMR spectra (CD_2Cl_2, 193K) of (NBu_4)[Pt(CNC)(CN)] (**2**) (above) and [Pt(CNC)(CN)Ag(PPh_3)] (**6**) (below).

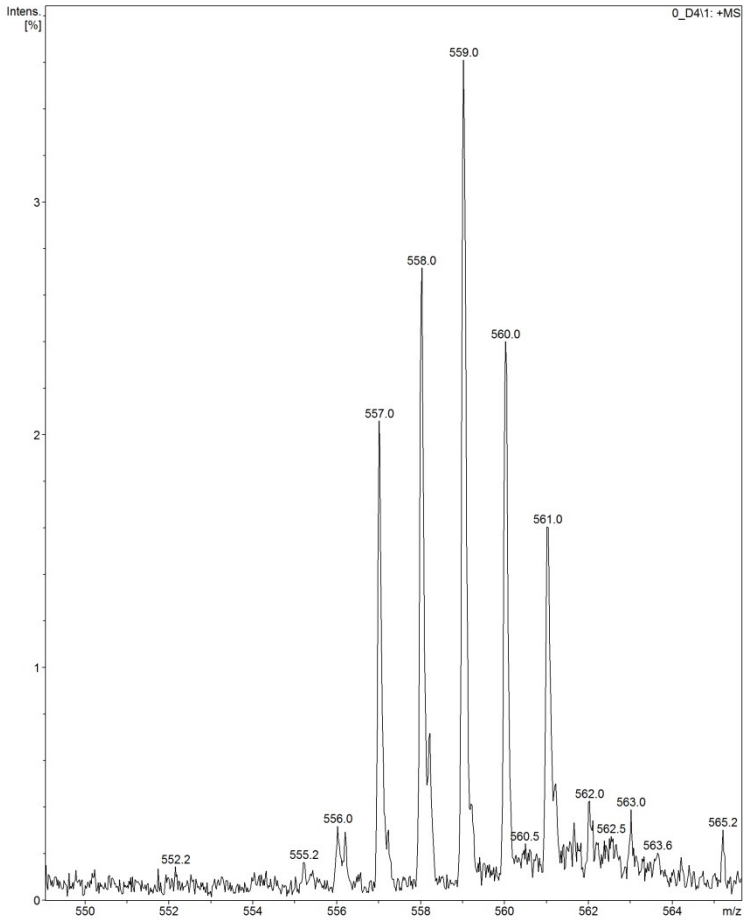

Figure S15. MS-MALDI+ (DIT) peak found for [Pt(CNC)(CN)Ag(PPh_3)] (**6**). This peak corresponds to [{PtAg(CNC)(CN)}]+H^+.

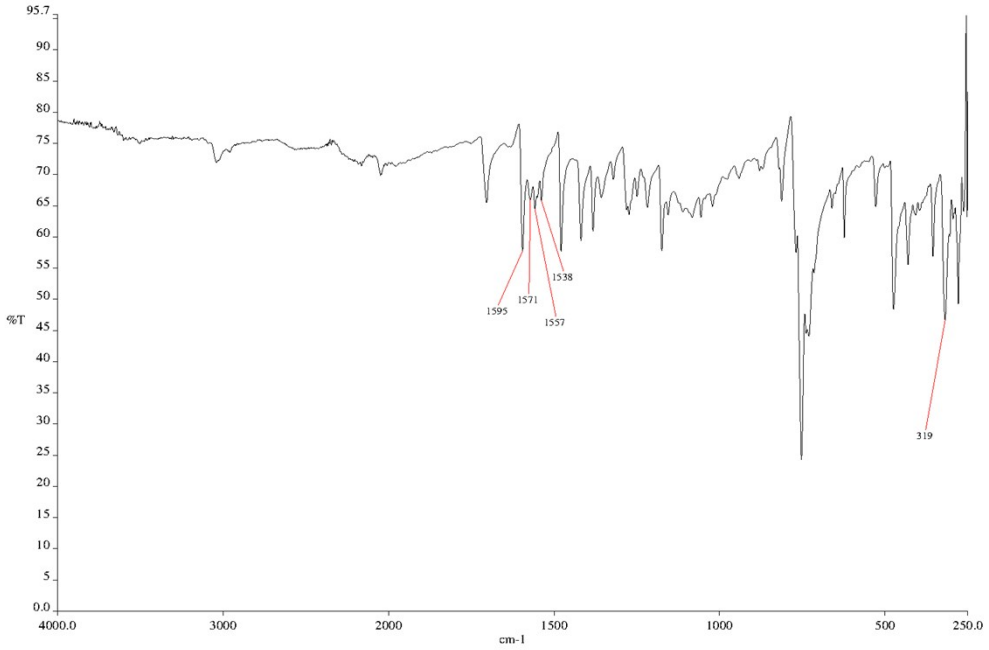

Figure S16. IR spectrum of [PtTl(CNC)(Cl)] (**7**).

Table S5. Relevant bond distances (Å) and angles (º) involving the metal atoms in the different arrangements for the units [PtTl(CNC)Cl] in **7.**

Pt(1A)−Tl(1A)	2.9044(9)	Pt(1A)−Tl(1D)	3.3644(9)
Tl(1A)−Pt(1B)	3.0376(9)	Pt(1B)−Tl(1B)	2.9906(9)
Tl(1B)−Pt(1C)	3.2124(9)	Pt(1C)−Tl(1C)	2.8882(9)
Tl(1C)−Pt(1D)	2.9883(10)	Pt(1D)−Tl(1D)#1	3.2309(9)
Pt(1E)−Tl(1E)	2.8563(9)	Pt(1F)−Tl(1F)	2.9409(9)
Tl(1A)−Pt(1A)−Tl(1D)	145.02(3)	Pt(1A)−Tl(1A)−Pt(1B)	130.67(3)
Tl(1B)−Pt(1B)−Tl(1A)	152.24(3)	Pt(1B)−Tl(1B)−Pt(1C)	139.48(3)
Pt(1B)−Cl(1B)−Tl(1A)	65.91(10)	Tl(1C)−Pt(1C)−Tl(1B)	148.16(3)
Pt(1C)−Tl(1C)−Pt(1D)	128.67(3)	Tl(1C)−Pt(1D)−Tl(1D)#1	131.76(3)
Pt(1D)#2−Tl(1D)−Pt(1A)	128.82(3)		

Symmetry transformations used to generate equivalent atoms are #1: x - 1, y, z; #2 x + 1, y, z.

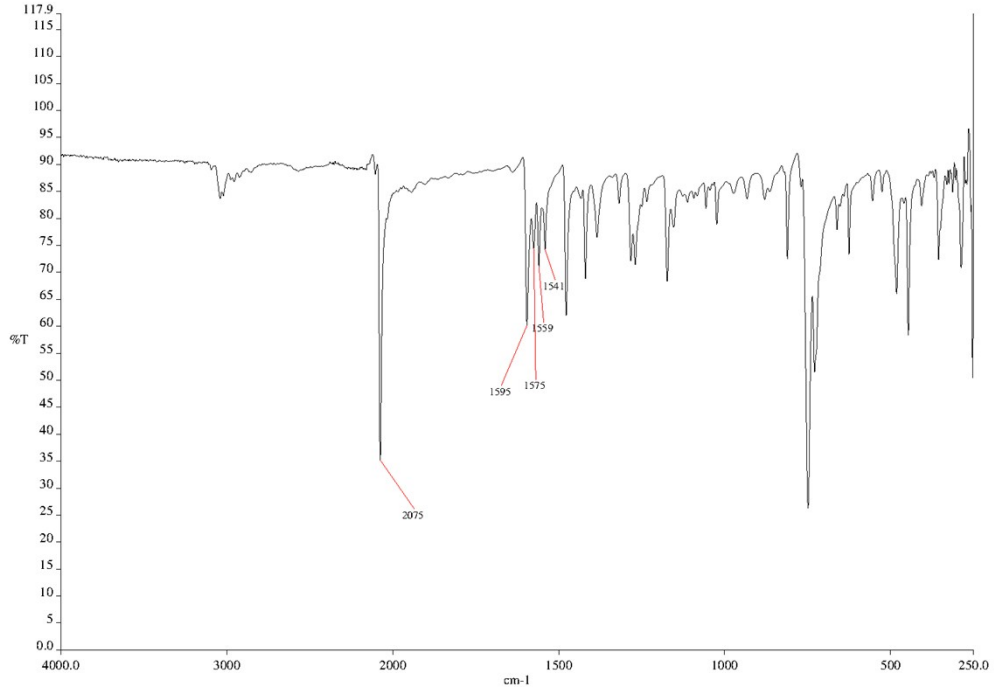

Figure S17. IR spectrum of [PtTl(CNC)(CN)] (**8**).

Table S6. Relevant bond distances (Å) and angles (º) for [PtTl(CNC)(CN)] (**8**)**.**

Pt(1A)−C(18A)	1.939(5)	Pt(1A)−N(1A)	2.012(4)
Pt(1A)−C(13A)	2.064(6)	Pt(1A)−C(1A)	2.066(6)
Pt(1A)−Tl(1A)	2.9241(3)	Tl(1A)−N(2A)#1	2.636(4)
Tl(1A)−N(2A)#2	2.653(5)	Pt(1B)−C(18B)	1.944(5)
Pt(1B)−N(1B)	2.010(4)	Pt(1B)−C(13B)	2.073(6)
Pt(1B)−C(1B)	2.074(5)	Pt(1B)−Tl(1B)	2.9207(3)
Tl(1B)−N(2B)#1	2.671(4)	Tl(1B)−N(2B)#4	2.683(5)
C(18A)−Pt(1A)−N(1A)	178.8(2)	C(18A)−Pt(1A)−C(13A)	98.9(2)
N(1A)−Pt(1A)−C(13A)	80.7(2)	C(18A)−Pt(1A)−C(1A)	99.5(2)
N(1A)−Pt(1A)−C(1A)	80.8(2)	C(13A)−Pt(1A)−C(1A)	161.5(2)
N(2A)#1−Tl(1A)−N(2A)#2	82.33(14)	C(18B)−Pt(1B)−N(1B)	178.54(19)
C(18B)−Pt(1B)−C(13B)	99.1(2)	N(1B)−Pt(1B)−C(13B)	80.6(2)
C(18B)−Pt(1B)−C(1B)	99.7(2)	N(1B)−Pt(1B)−C(1B)	80.6(2)
C(13B)−Pt(1B)−C(1B)	161.2(2)	N(2B)#1−Tl(1B)−N(2B)#4	85.37(15)

Symmetry transformations used to generate equivalent atoms are #1: x - 1, y, z; #2: -x + 1, -y + 1, -z + 2; #3: -x, -y + 1, -z + 1.

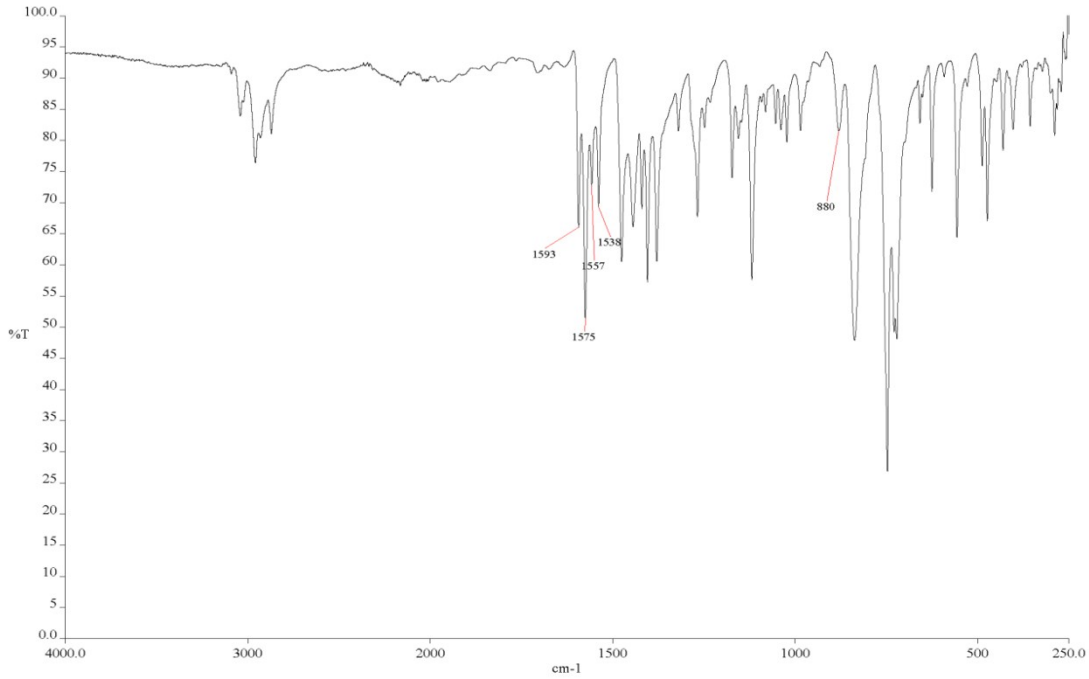

Figure S18. IR spectrum of $(NBu_4)[\{Pt(CNC)(S\text{-}2Py)\}_2Tl]$ (**9**)

Table S7. Relevant bond distances (Å) and angles (º) for $(NBu_4)[\{Pt(CNC)(S\text{-}2py)\}_2Tl]\cdot CH_2Cl_2$ (**9**).

Pt(1)−N(1)	1.997(4)	Pt(1)−C(7)	2.055(5)
Pt(1)−C(13)	2.061(5)	Pt(1)−S(1)	2.2876(11)
Pt(1)−Tl	2.8953(2)	Pt(2)−N(3)	1.995(3)
Pt(2)−C(29)	2.061(5)	Pt(2)−C(35)	2.071(4)
Pt(2)−S(2)	2.2836(11)	Pt(2)−Tl	2.9184(2)
Tl−N(2)	2.671(4)	Tl−N(4)	2.710(4)
N(1)−Pt(1)−C(7)	80.68(18)	N(1)−Pt(1)−C(13)	80.83(18)
C(7)−Pt(1)−C(13)	161.51(18)	N(1)−Pt(1)−S(1)	169.66(11)
C(7)−Pt(1)−S(1)	96.04(14)	C(13)−Pt(1)−S(1)	102.17(13)
N(3)−Pt(2)−C(29)	80.96(17)	N(3)−Pt(2)−C(35)	80.38(17)
C(29)−Pt(2)−C(35)	161.31(17)	N(3)−Pt(2)−S(2)	169.05(10)
C(29)−Pt(2)−S(2)	96.64(12)	C(35)−Pt(2)−S(2)	101.89(13)
Pt(1)−Tl−Pt(2)	165.58(1)	N(2)−Tl−N(4)	104.92(11)

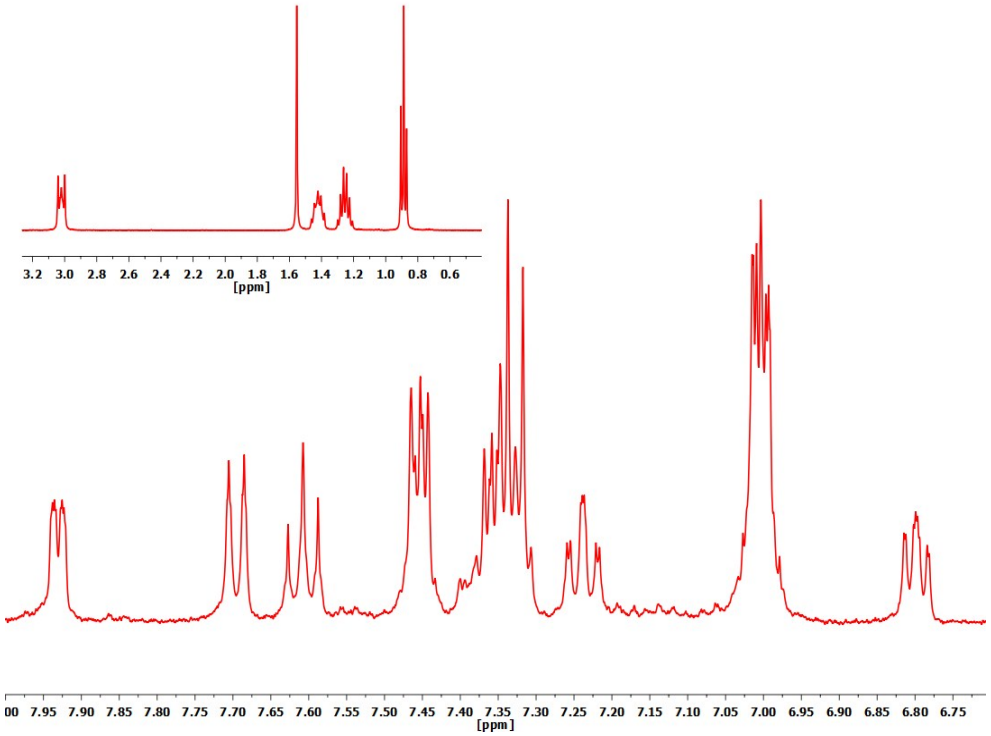

Figure S19. ^{1}H NMR spectrum (CD_2Cl_2, room temperature) of solutions of $(NBu_4)[\{Pt(CNC)(S\text{-}2Py)\}_2Tl]$ (**9**).

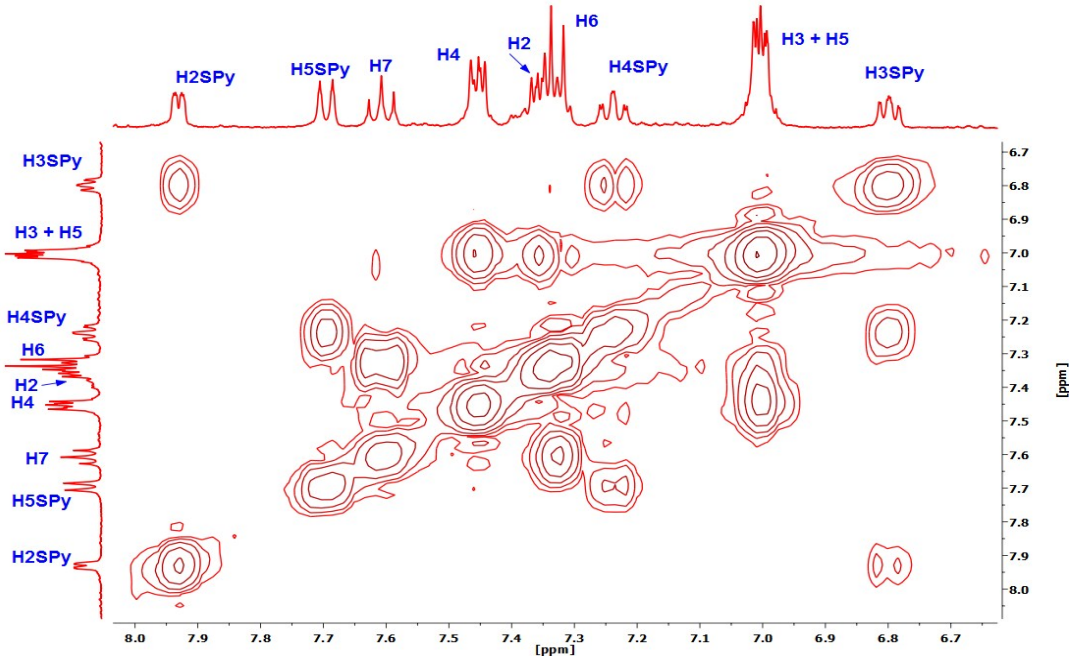

Figure S20. COSY (^{1}H-^{1}H) (CD_2Cl_2, RT) spectrum of solutions of $(NBu_4)[\{Pt(CNC)(S\text{-}2Py)\}_2Tl]$ (**9**).

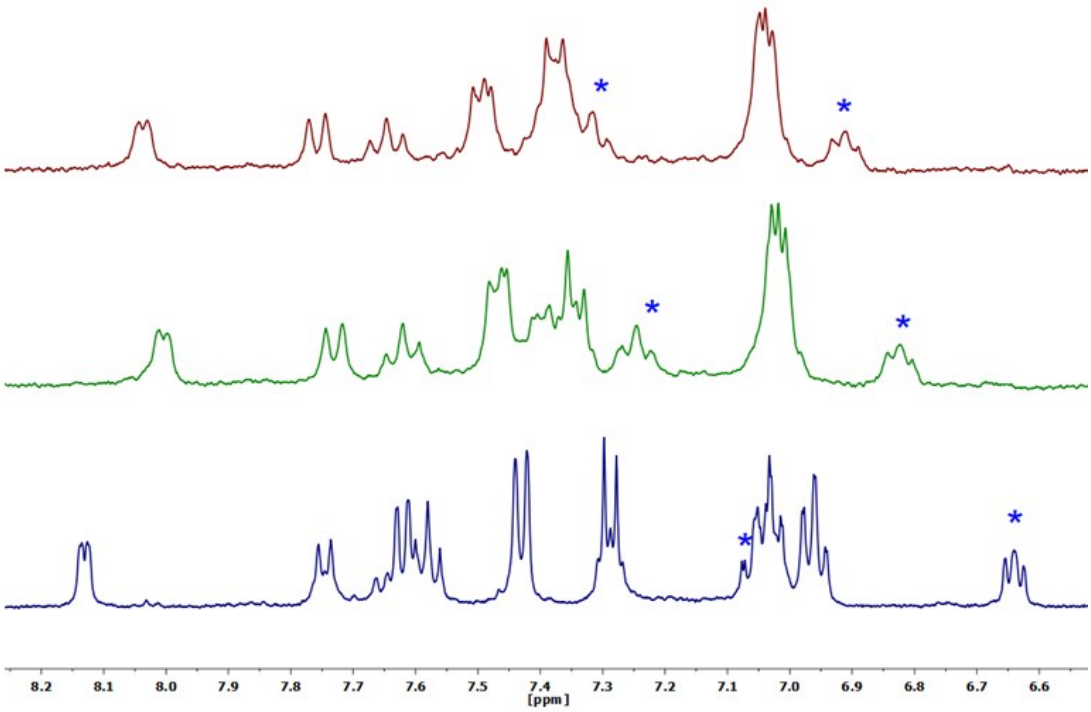

Figure S21. ^{1}H NMR spectra of solutions of $(NBu_4)[\{Pt(CNC)(S\text{-}2Py)\}_2Tl]$ (**9**) (above), $(NBu_4)[Pt(CNC)(S\text{-}2Py)]$ (**3**) (below) and a mixture of both (middle) (CD_2Cl_2, room temperature).

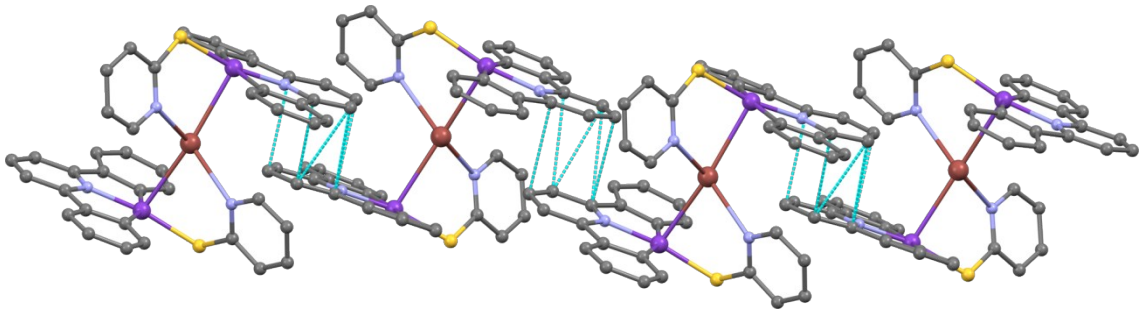

Figure S22. Supramolecular arrangement found in the crystal structure of $(NBu_4)[\{Pt(CNC)(S\text{-}2py)\}_2Tl]$ (**9**) showing the π···π intermolecular interactions.

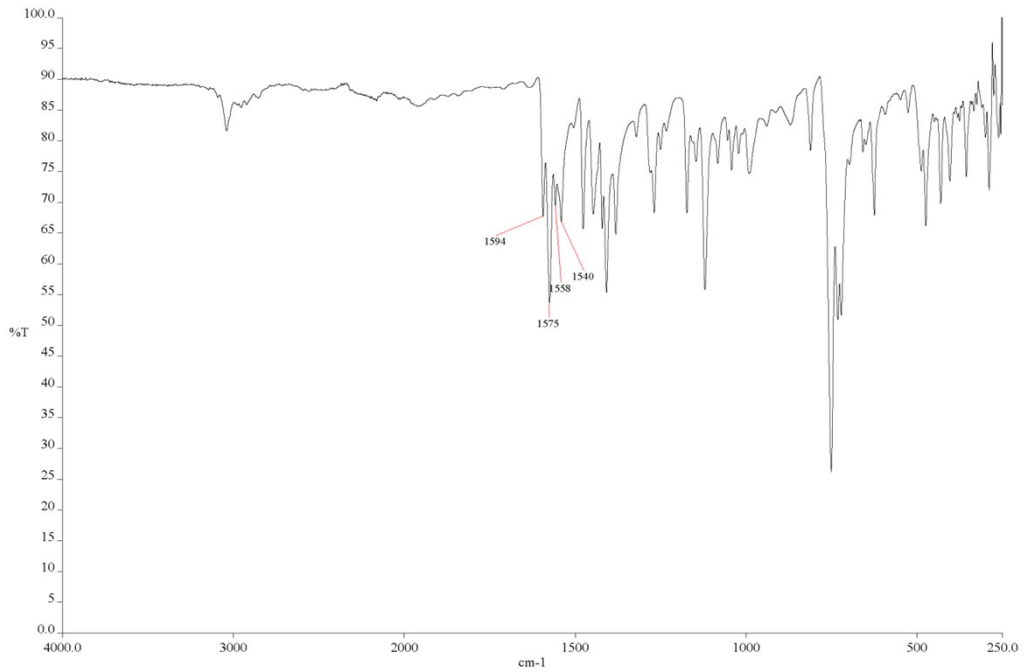

Figure S23. IR spectrum of [PtTl(CNC)(S-2py)] (**10**).

Table S8**.** Relevant bond distances (Å) and angles (º) for [PtTl(CNC)(S-2py)] (**10**)**.**

Pt(1)−N(1)	2.007(13)	Pt(1)−C(7)	2.059(18)
Pt(1)−C(13)	2.10(2)	Pt(1)−S(1)	2.284(4)
Pt(1)−Tl(1)	2.8324(9)	Pt(1)−Tl(2)	2.9991(9)
Pt(2)−N(3)	2.002(14)	Pt(2)−C(29)	2.067(17)
Pt(2)−C(35)	2.078(17)	Pt(2)−S(2)	2.286(5)
Pt(2)−Tl(2)	2.8222(9)	Pt(3)−N(5)	2.013(12)
Pt(3)−C(57)	2.070(19)	Pt(3)−C(51)	2.080(19)
Pt(3)−S(3)	2.320(4)	Pt(3)−Tl(3)#1	2.8839(9)
Pt(3)−Tl(3)	2.9183(9)	Tl(1)−N(2)	2.642(17)
Tl(2)−N(4)	2.586(15)	Tl(3)−N(6)	2.673(14)
Tl(1)−Pt(1)−Tl(2)	158.64(3)	Tl(3)#1−Pt(3)−Tl(3)	161.48(3)
Pt(2)−Tl(2)−Pt(1)	155.90(3)	Pt(3)#2−Tl(3)−Pt(3)	144.30(3)

Symmetry transformations used to generate equivalent atoms are #1: x − 1/2, −y + 3/2, −z + 2; #2: x + 1/2, −y + 3/2, −z + 2.

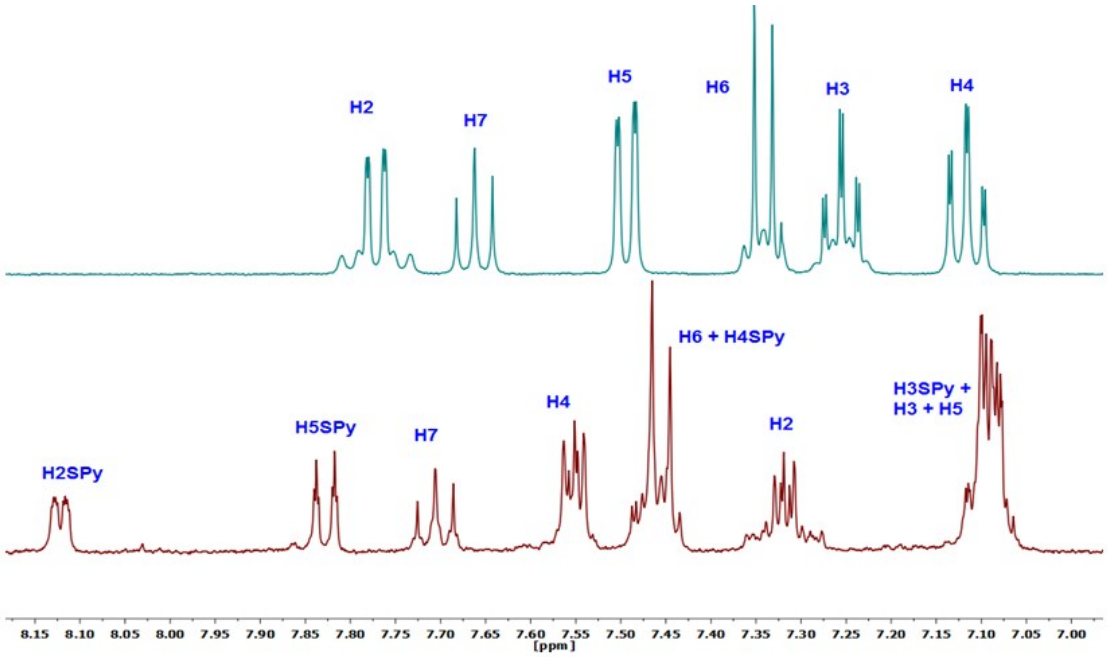

Figure S24. ^{1}H NMR spectra (CD_2Cl_2, room temperature) of the starting material [Pt(CNC)(dmso)] (above) and [PtTl(CNC)(S-2py)] (**10**) (below).

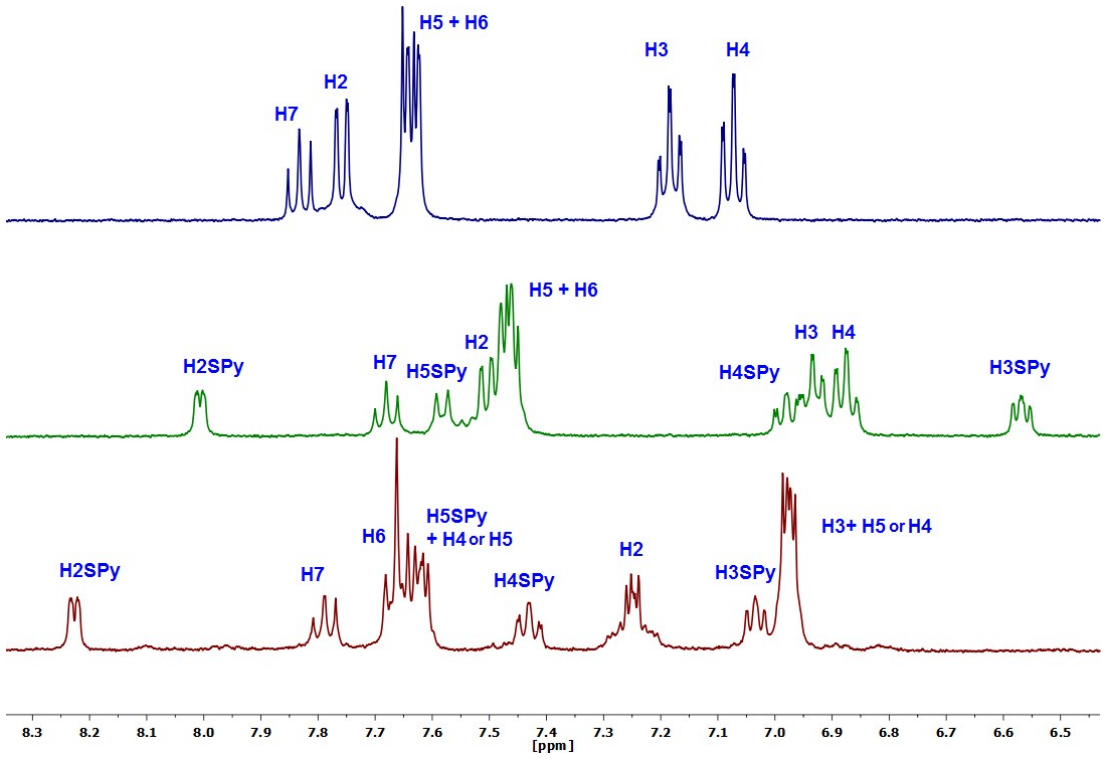

Figure S25. ^{1}H NMR spectra (dmso-d_6, room temperature) of the starting material [Pt(CNC)(dmso)] (above), $[Pt(CNC)(S\text{-}2py)]^-$ (middle) and [PtTl(CNC)(S-2py)] (**10**) (below).

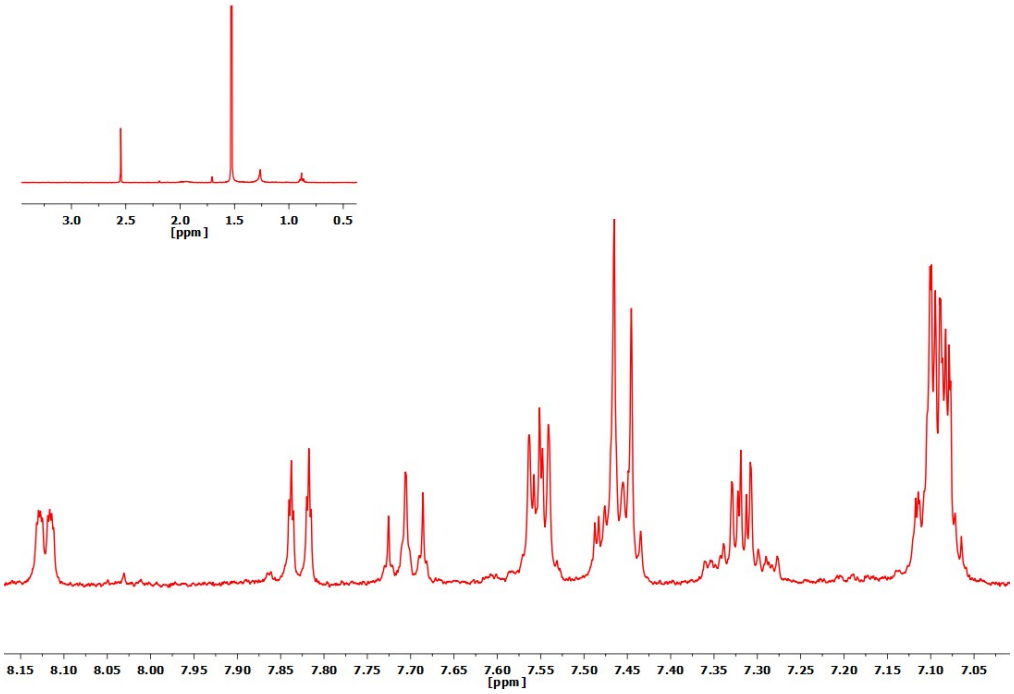

Figure S26. ^{1}H NMR (CD_2Cl_2, RT) spectrum of complex [PtTl(CNC)(S-2py)] (**10**).

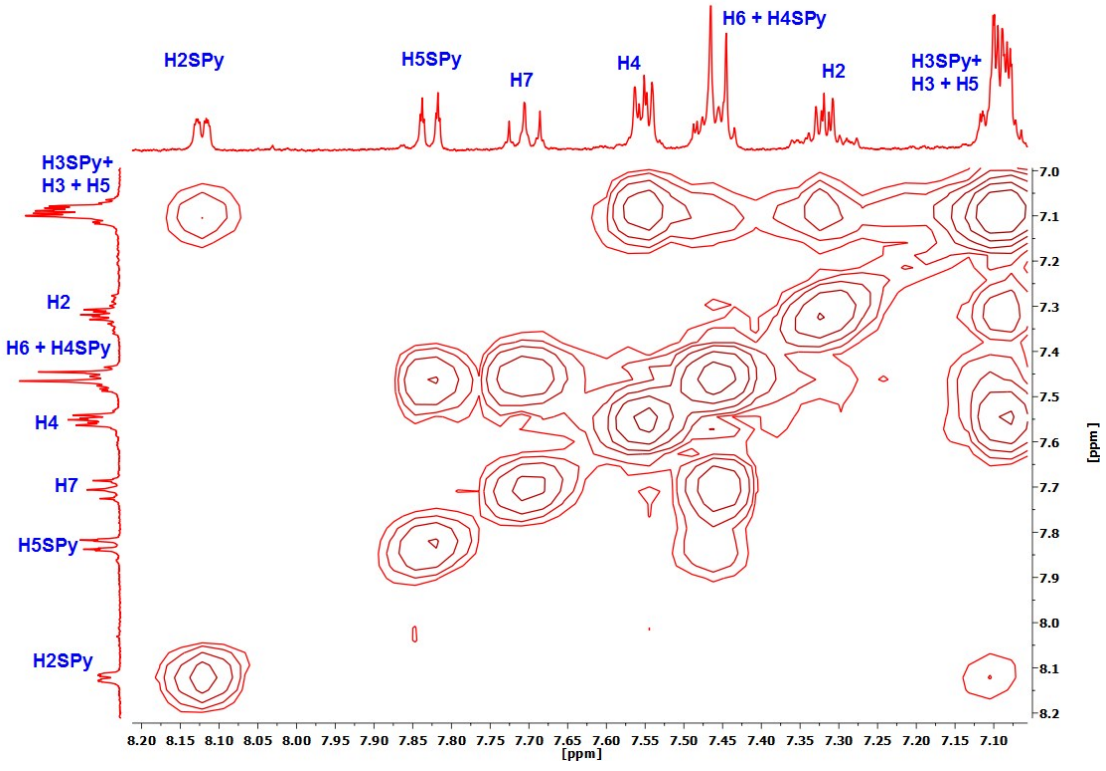

Figure S27. COSY (^{1}H-^{1}H) (CD_2Cl_2, RT) spectrum of complex [PtTl(CNC)(S-2py)] (**10**).

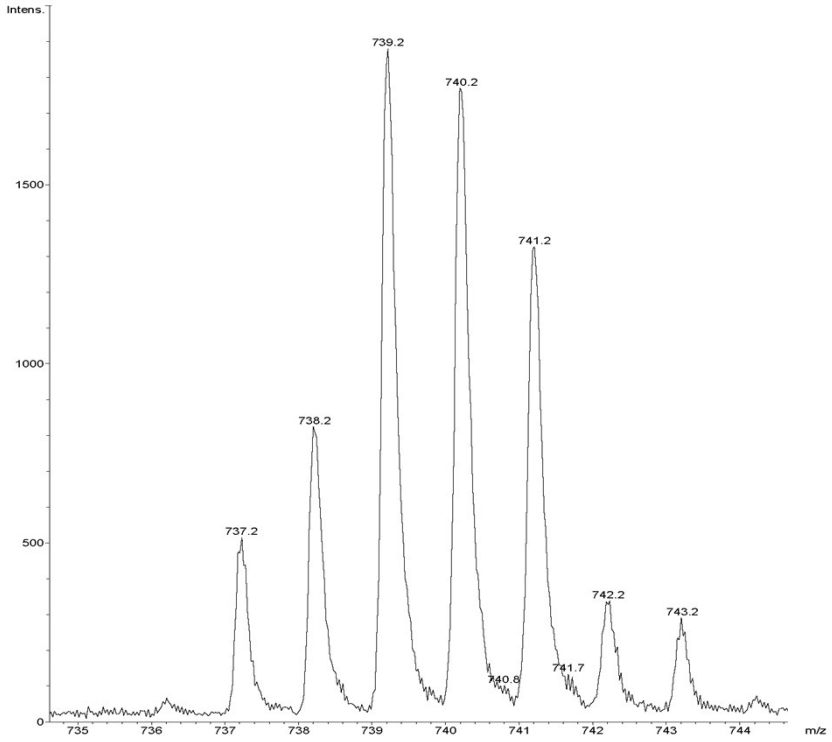

Figure S28. MS-MALDI+ (DIT) peak of complex [PtTl(CNC)(S-2py)] (**10**).

Table S9. Crystal data and structure refinement for complexes (NBu_4)[Pt(CNC)Cl] (**1**), .[{Pt(CNC)(μ-CN)}$_4$Ag$_4$]·3DMF (**4**·3DMF), [{Pt(CNC)(S-2py)}$_2$Ag$_2$]·CH_2Cl_2 (**5**·CH_2Cl_2) and [{Pt(CNC)(μ-CN)}$_2${Ag(PPh_3)}$_2$]·CH_2Cl_2 (**6**·CH_2Cl_2).

	1	**4**·3DMF	**5**·CH_2Cl_2	**6**·CH_2Cl_2
Formula	$C_{33}H_{47}ClN_2Pt$	$C_{72}H_{44}Ag_4N_8Pt_4$ ·3DMF	$C_{44}H_{30}Ag_2N_4Pt_2S_2$ ·CH_2Cl_2	$C_{72}H_{52}Ag_2N_4P_2Pt_2$ ·CH_2Cl_2
M_t	702.27	2452.28	1625.54	1725.96
Crystal system	Monoclinic	Monoclinic	Monoclinic	Monoclinic
Space group	*Pc*	$P2_1/c$	$P2_1/n$	$P2_1/n$
a/Å	9.8461(1)	22.7941(4)	10.5025(4)	17.7051(4)
b/Å	8.5788(1)	14.0196(2)	22.8137(11)	16.6937(3)
c/Å	18.1409(2)	24.1626(5)	16.7653(5)	22.3552(5)
β/º	99.300(1)	112.702(2)	97.478(3)	110.664(3)
V/Å^3	1512.18(3)	7123.3(2)	3982.8(3)	6182.3(3)
Z	2	4	4	4
D_c/g cm^{-3}	1.542	2.287	2.284	1.854
T/K	100(1)	100(1)	100(1)	100(1)
μ/mm^{-1}	4.752	8.958	8.251	5.321
F(000)	708	4608	2584	3336
2*θ* range/º	8.4-57.8	8.7-58.8	6.6-52.0	8.4-59.4
Collected reflections	17133	60680	18849	27936

Unique reflections	6873	15948	7788	15404
R_{int}	0.0274	0.0514	0.0505	0.0435
R_1, wR_2[a] ($I > 2\sigma(I)$)	0.0221, 0.0465	0.0340, 0.0728	0.0429, 0.0950	0.0478, 0.0850
R_1, wR_2[a] (all data)	0.0261, 0.0489	0.0481, 0.0807	0.0574, 0.1026	0.0706, 0.0949
Abs. struc. par.	-0.018(5)	-	-	-
GOF (F^2)[b]	1.001	1.032	1.032	1.042

[a] $R_1 = \sum(|F_o| - |F_c|) / \sum |F_o|$. $wR_2 = [\sum w (F_o^2 - F_c^2)^2 / \sum w(F_o^2)^2]^{1/2}$. [b] Goodness-of-fit = $[\sum w (F_o^2 - F_c^2)^2 / (n_{obs} - n_{param})]^{1/2}$

Table S10. Crystal data and structure refinement for complexes [PtTl(CNC)Cl]·0.28Me_2CO·0.18H_2O (**7**·0.28Me_2CO·0.18H_2O), [PtTl(CNC)(CN)]·DMF (**8**·DMF), (NBu_4)[{Pt(CNC)(S-2py)}$_2$Tl]·CH_2Cl_2 (**9**·CH_2Cl_2) and [PtTl(CNC)(S-2py)] (**10'**).

	7·0.28Me_2CO·0.18H_2O	**8**·DMF	**9**·CH_2Cl_2	**10**
Formula	$C_{17}H_{11}ClNPtTl$ ·0.28Me_2CO·0.18H_2O	$C_{18}H_{11}N_2PtTl$ ·DMF	$C_{44}H_{30}N_4Pt_2S_2Tl$ ·CH_2Cl_2	$C_{22}H_{15}N_2PtSTl$
M_t	684.09	727.84	1600.77	738.67
Crystal system	Monoclinic	Triclinic	Monoclinic	Orthorhombic
Space group	$P2_1/n$	P-1	$P2_1/c$	$P2_12_12_1$
a/Å	21.1234(4)	5.9405(1)	13.8571(2)	10.8874(2)
b/Å	19.1822(4)	15.5744(3)	24.0654(5)	22.7857(6)
c/Å	24.3466(5)	22.0135(4)	17.5724(4)	23.2532(5)
α/º	90	70.343(2)	90	90
β/º	102.189(2)	88.302(1)	103.331(2)	90
γ/º	90	79.253(1)	90	90
V/Å^3	9642.7(4)	1883.16(6)	5702.1(2)	5768.6(2)
Z	24	4	4	12
D_c/g cm^{-3}	2.828	2.567	1.865	2.552
T/K	100(1)	100(1)	100(1)	100(1)
μ/mm^{-1}	18.875	15.982	7.924	15.754
F(000)	7368	1328	3088	4032

2θ range/^{o}	8.6-50.0	9.0-58.5	6.4-60.3	6.4-62.5
Collected reflections	54965	40943	49714	35383
Unique reflections	16855	9120	14927	16324
R_{int}	0.0650	0.0346	0.0410	0.0709
R_1, wR_2[a] ($I > 2\sigma(I)$)	0.0648, 0.1582	0.0279, 0.0561	0.0336, 0.0684	0.0553, 0.1015
R_1, wR_2[a] (all data)	0.0860, 0.1765	0.0390, 0.0596	0.0464, 0.0731	0.0796, 0.1142
GOF (F^2)[b]	1.050	1.055	1.065	1.012

[a] $R_1 = \sum(|F_o| - |F_c|) / \sum |F_o|$. $wR_2 = [\sum w (F_o^2 - F_c^2)^2 / \sum w(F_o^2)^2]^{1/2}$. [b] Goodness-of-fit = $[\sum w (F_o^2 - F_c^2)^2 / (n_{obs} - n_{param})]^{1/2}$